

A DETECTOR OF GRAVITATIONAL WAVES BASED ON COUPLED MICROWAVE CAVITIES

Ph. Bernard

CERN, CH-1211, Geneva 23, Switzerland

A. Chincarini, G. Gemme,* and R. Parodi

INFN-Sezione di Genova, via Dodecaneso 33, I-16146 Genova, Italy

E. Picasso

Scuola Normale Superiore, Piazza dei Cavalieri 7, I-56126, Pisa, Italy

(Dated: March 4, 2002)

Abstract

Since 1978 superconducting coupled cavities have been proposed as sensitive detector of gravitational waves. The interaction of the gravitational wave with the cavity walls, and the resulting motion, induces the transition of some electromagnetic energy from an initially excited cavity mode to an empty one. The energy transfer is maximum when the frequency of the wave is equal to the frequency difference of the two cavity modes. In this paper the basic principles of the detector are discussed. The interaction of a gravitational wave with the cavity walls is studied in the proper reference frame of the detector, and the coupling between two electromagnetic normal modes induced by the wall motion is analyzed in detail. Noise sources are also considered; in particular the noise coming from the brownian motion of the cavity walls is analyzed. Some ideas for the development of a realistic detector of gravitational waves are discussed; the outline of a possible detector design and its expected sensitivity are also shown.

PACS numbers: 07.57.-c; 04.80.Nn; 95.55.Ym

I. INTRODUCTION

In a series of papers it was studied how the effects due to the interaction between the gravitational and the electromagnetic fields could be used to detect gravitational waves [1, 2]. The proposed detector exploits the energy transfer induced by the gravitational wave between two levels of an electromagnetic resonator, whose frequencies ω_1 and ω_2 are both much larger than the angular frequency Ω of the g.w. and satisfy the resonance condition $|\omega_2 - \omega_1| = \Omega$.¹ In the scheme suggested by Bernard et al. the two levels are obtained by coupling

*Corresponding author; Electronic address: gianluca.gemme@ge.infn.it

¹ The interaction between the g.w. and the detector is characterized by a transfer of energy and of angular momentum. Since the elicity of the g.w., i.e. the angular momentum along the direction of propagation, is 2, it can induce a transition between the two levels provided their angular momenta differ by 2; this can be achieved by putting the two cavities at right angle or by a suitable polarization of the electromagnetic field inside the resonator.

two identical high frequency cavities²; the angular frequency ω_1 is the frequency of the level symmetrical in the fields of the two cavities, and ω_2 is that of the antisymmetrical one. The frequency difference between the symmetric and the antisymmetric level is determined by the coupling, and can be adjusted by a careful resonator design. Since the detector sensitivity is proportional to the square of the resonator quality factor, superconducting cavities should be used for maximum sensitivity.

The power transfer between the levels of a resonator made up of two pill-box cavities, mounted *end-to-end* and coupled by a small circular aperture in their common endwall, was checked in a series of experiments by Melissinos et al., where the perturbation of the resonator volume was induced by a piezoelectric crystal [3, 4]. Recently the experiment was repeated by our group with an improved experimental set-up; we obtained a sensitivity to fractional deformations of the resonator length as small as $\delta\ell/\ell \approx 10^{-20} \text{ Hz}^{-1/2}$ [5].

In this paper we shall discuss the mechanism of the interaction of a gravitational wave with a detector based on two coupled resonant cavities. In previous works this issue was discussed using the concept of a dielectric tensor associated with the gravitational wave [6]. The interaction was analyzed in the reference frame where the resonator walls were *at rest* even in presence of a gravitational perturbation. We shall analyze the effect in the proper reference frame attached to the detector and we shall therefore consider the interaction between the wave and the field stored inside the resonator due to the coupling of the g.w. with the *mechanical* structure of the detector [7].

The paper will be organized as follows: in section II the problem of finding the electromagnetic fields in a closed volume with time-varying boundary conditions is studied, and an approximate expression of the normal modes in a perturbed resonator is worked out. In section III we shall analyze the interaction of a g.w. with the mechanical structure of the detector; we shall see that the transfer of energy between a mechanical and an electromagnetic oscillation depends both on the electromagnetic field distribution inside the resonator and on the resonator geometry and mechanical properties. In section IV we shall discuss some ideas for the development of a realistic gravitational wave detector based on spherical microwave cavities. Afterwards the coupled equations of motion for the fields in a perturbed resonator are worked out and solved. In section VIII the issue of the thermal noise of the detector's walls is studied; other noise contributions are also considered. Finally, in the last section, the expected sensitivity of some detector configuration is shown and discussed.

II. ELECTROMAGNETIC FIELD IN A RESONATOR WITH PERTURBED BOUNDARIES

To study the mechanism of the energy transfer between the two levels of an electromagnetic resonator perturbed by a gravitational wave we shall follow classic electromagnetic theory. We shall make use of the fact that any field configuration inside the resonator can be expressed as the superposition of the electromagnetic normal modes of the given resonator [8].

If no sources are present, the electromagnetic field in vacuum is determined by the equa-

² Throughout this paper, we shall call *resonator* the whole detector made up of two coupled *cavities*; e.g. we shall speak about one resonator composed by two coupled spherical cavities.

tions:

$$\vec{\nabla} \cdot \vec{E} = 0 \quad (1)$$

$$\vec{\nabla} \cdot \vec{H} = 0 \quad (2)$$

$$\vec{\nabla} \wedge \vec{E} + \mu_0 \frac{\partial \vec{H}}{\partial t} = 0 \quad (3)$$

$$\vec{\nabla} \wedge \vec{H} - \epsilon_0 \frac{\partial \vec{E}}{\partial t} = 0 \quad (4)$$

As can be easily verified, eqs. (1)–(4) are automatically satisfied if the fields satisfy the wave equations:

$$\nabla^2 \vec{E} - \frac{1}{c^2} \frac{\partial^2 \vec{E}}{\partial t^2} = 0 \quad (5)$$

$$\nabla^2 \vec{H} - \frac{1}{c^2} \frac{\partial^2 \vec{H}}{\partial t^2} = 0 \quad (6)$$

with $c = (\mu_0 \epsilon_0)^{-1/2}$.

Let us assume that the field is contained in a resonator with perfectly conducting walls. If we impose boundary conditions on the fields, the solution of the wave equations (5)–(6) will have an infinite discrete set of normal-mode solutions orthogonal to one another and complete, in the sense that any arbitrary field in the resonator can be expressed as a sum of these normal modes with suitable amplitudes. The amplitudes of each mode can then be used to describe the field in the resonator.

By the familiar procedure of separation of variables we may assume a solution of eqs. (5)–(6) of the form:

$$\vec{E}(\vec{r}, t) = \sum_{n=0}^{\infty} \mathcal{E}_n(t) \vec{E}_n(\vec{r}) \quad (7)$$

and

$$\vec{H}(\vec{r}, t) = \sum_{n=0}^{\infty} \mathcal{H}_n(t) \vec{H}_n(\vec{r}) \quad (8)$$

where we have defined:

$$\mathcal{E}_n(t) \equiv \sqrt{\epsilon_0} \int_V \vec{E} \cdot \vec{E}_n dV \quad (9)$$

and

$$\mathcal{H}_n(t) \equiv \sqrt{\mu_0} \int_V \vec{H} \cdot \vec{H}_n dV \quad (10)$$

where the integrals are performed over the resonator volume.

We require that at the walls the tangential component of \vec{E} and the normal component of \vec{H} vanish. With this assumption the functions $\vec{E}_n(\vec{r})$ and $\vec{H}_n(\vec{r})$ satisfy the equations:

$$k_n \vec{E}_n = \vec{\nabla} \wedge \vec{H}_n \quad (11)$$

$$k_n \vec{H}_n = \vec{\nabla} \wedge \vec{E}_n \quad (12)$$

where $k_n = \omega_n/c$ is the propagation constant associated with the n_{th} mode.

It can be proved that the normal modes \vec{E}_n and \vec{H}_n have orthogonality properties of the form

$$\int_V \vec{E}_n \cdot \vec{E}_m dV = \delta_{nm} \quad (13)$$

$$\int_V \vec{H}_n \cdot \vec{H}_m dV = \delta_{nm} \quad (14)$$

For a cubical resonator the functions $\vec{E}_n(\vec{r})$ and $\vec{H}_n(\vec{r})$ are $\sin(\vec{k}_n \cdot \vec{r})$ and $\cos(\vec{k}_n \cdot \vec{r})$. For other geometries they will be other complete sets of functions. The boundary conditions and geometry determine the different modes which are distinguished by the index n . In general three numbers are needed to specify a mode; n is an abbreviation for this set of numbers.

Let us now expand the fields \vec{E} , \vec{H} in terms of the orthogonal functions \vec{E}_n and \vec{H}_n ; when we substitute these expansions in Maxwell's equations and equate coefficients, so as to get the differential equations satisfied by the various coefficients, we find that equations (1) and (2) are automatically satisfied. From equations (3) and (4) we find the following equations for the expansion coefficients:

$$\frac{d\mathcal{H}_n(t)}{dt} - \omega_n \mathcal{E}_n(t) = -\frac{\omega_n}{\mathcal{Q}_n} \mathcal{H}_n(t) \quad (15)$$

$$\frac{d\mathcal{E}_n(t)}{dt} + \omega_n \mathcal{H}_n(t) = 0 \quad (16)$$

We have taken into account the dissipation arising from the finite conductivity of the walls introducing the electromagnetic quality factor [8]:

$$\mathcal{Q}_n = \frac{\omega_n \mu_0 \int_V H_n^2 dV}{R_s \int_S H_n^2 dS} = \frac{G_n}{R_s} \quad (17)$$

R_s is the material-dependent surface resistance of the walls, and the geometric factor G_n of the n_{th} mode is defined as:

$$G_n = \omega_n \mu_0 \frac{\int_V H_n^2 dV}{\int_S H_n^2 dS} \quad (18)$$

As can readily be seen, equations (15)–(16) for the field expansion coefficients are decoupled: the modes are independent from one another and behave as simple damped harmonic oscillators.

A. Perturbation of boundaries

Let us suppose that the resonator's boundary is perturbed so that the eigenvalues and eigenfunctions of the perturbed resonator differ but little from those of the original one. The perturbation method allows to find the eigenvalues and eigenfunctions of the perturbed problem from the knowledge of the original ones. It basically consists in expanding in power series of a perturbation parameter σ the new modes and frequencies [9]:

$$\begin{aligned} \vec{E}'_n(\vec{r}) &= \vec{E}_n(\vec{r}) + \sigma \vec{e}_n(\vec{r}) + \mathcal{O}(\sigma^2) \\ \vec{H}'_n(\vec{r}) &= \vec{H}_n(\vec{r}) + \sigma \vec{h}_n(\vec{r}) + \mathcal{O}(\sigma^2) \\ k'_n &= k_n + \sigma \kappa_n + \mathcal{O}(\sigma^2) \end{aligned} \quad (19)$$

In the perturbed resonator we shall have:

$$\vec{E}(\vec{r}, t) = \sum_{n=0}^{\infty} \tilde{\mathcal{E}}_n(t) \vec{E}'_n(\vec{r}) \quad (20)$$

and

$$\vec{H}(\vec{r}, t) = \sum_{n=0}^{\infty} \tilde{\mathcal{H}}_n(t) \vec{H}'_n(\vec{r}) \quad (21)$$

with:

$$\tilde{\mathcal{E}}_n(t) \equiv \sqrt{\epsilon_0} \int_{V'} \vec{E} \cdot \vec{E}'_n dV \quad (22)$$

and

$$\tilde{\mathcal{H}}_n(t) \equiv \sqrt{\mu_0} \int_{V'} \vec{H} \cdot \vec{H}'_n dV \quad (23)$$

where the integrals are now performed over the perturbed volume V' .

The perturbed modes will satisfy the following equations:

$$k'_n \vec{E}'_n = \vec{\nabla} \wedge \vec{H}'_n \quad (24)$$

$$k'_n \vec{H}'_n = \vec{\nabla} \wedge \vec{E}'_n \quad (25)$$

When the expansions (19) are inserted into the equations (24) we obtain a series of equations determining the various terms of the expansion (19). In the first order approximation, the perturbed fields may be written:

$$\sigma \vec{e}_n(\vec{r}) = \sum_{m=1}^{\infty} A_{nm} \vec{E}_m(\vec{r}) \quad (26)$$

$$\sigma \vec{h}_n(\vec{r}) = -\frac{1}{2} \mathcal{C}_{nn} \vec{H}_n(\vec{r}) + \sum_{m=1}^{\infty} B_{nm} \vec{H}_m(\vec{r}) \quad (27)$$

$$\sigma \kappa_n = -\frac{1}{2} k_n \mathcal{C}_{nn} \quad (28)$$

where the sums have to be performed for $n \neq m$. The expansion coefficients have the form [9]:

$$A_{nm} = \frac{k_m k_n}{k_m^2 - k_n^2} \mathcal{C}_{nm} \quad (29)$$

$$B_{nm} = \frac{k_n^2}{k_m^2 - k_n^2} \mathcal{C}_{nm} \quad (30)$$

with

$$\mathcal{C}_{nm} = \int_{\mathcal{V}} (\vec{H}_n \cdot \vec{H}_m - \vec{E}_n \cdot \vec{E}_m) dV \quad (31)$$

where $\mathcal{V} = V' - V$ is the (algebraic) difference between the perturbed and the original volume.³

The calculation of the coupling coefficient \mathcal{C}_{nm} depends on how the resonator is deformed by an external force. For this reason in the next section we shall briefly review the study of the mechanical behaviour of a body under the influence of an external force.

³ The derivation of the eigenmodes and eigenvalues of the perturbed resonator has been made assuming a *static* perturbation; in the following we shall assume that it is also correct for a perturbation which has a rate of change much slower than the e.m. field characteristic frequency.

III. ANALYSIS OF THE MECHANICAL RESPONSE OF THE DETECTOR

The interaction of a gravitational wave with the mechanical structure of the detector can be studied by means of classical, non-relativistic, linear elasticity theory [10, 11]. If $\vec{u}(\vec{r})$ denotes the displacement of the mass element at point \vec{r} , relative to the centre of mass of the body in its unperturbed state, and $\vec{f}(\vec{r}, t)$ is the volume force density which acts on the body, the displacement is the solution of the system of partial differential equations:

$$\rho \frac{\partial^2 \vec{u}}{\partial t^2} - \mu \nabla^2 \vec{u} - (\lambda + \mu) \vec{\nabla}(\vec{\nabla} \cdot \vec{u}) = \vec{f}(\vec{r}, t) \quad (32)$$

with suitable boundary and initial conditions. $\rho(\vec{r})$ is the mass density of the body and λ and μ are the material's elastic Lamé coefficients. In the following we shall adopt null initial conditions:

$$\vec{u}(\vec{r}, 0) = \frac{\partial \vec{u}}{\partial t}(\vec{r}, 0) = 0 \quad (33)$$

The expansion theorem [12] states that the displacement of a system in response to an applied force is equal to the superposition of the normal modes $\vec{\xi}_\alpha(\vec{r})$ of the system⁴:

$$\vec{u}(\vec{r}, t) = \sum_{\alpha=1}^{\infty} \vec{\xi}_\alpha(\vec{r}) q_\alpha(t) \quad (34)$$

The normal modes $\vec{\xi}_\alpha(\vec{r})$ are the eigen-solutions to

$$\mu \nabla^2 \vec{\xi}_\alpha + (\lambda + \mu) \vec{\nabla}(\vec{\nabla} \cdot \vec{\xi}_\alpha) = -\omega_\alpha^2 \rho \vec{\xi}_\alpha \quad (35)$$

with boundary conditions; here α is an index, or set of indices, labelling the mode of frequency ω_α . The modes are normalized so that

$$\int_{Vol} \vec{\xi}_\alpha(\vec{r}) \cdot \vec{\xi}_\beta(\vec{r}) \rho(\vec{r}) dV = M_\alpha \delta_{\alpha\beta} \quad (36)$$

where M_α is the reduced mass of the α mode. For a homogeneous system $M_\alpha \equiv M$, where M is the mass of the system.

$q_\alpha(t)$ is the generalized coordinate of the α mode, obeying the dynamical equation of motion:

$$\ddot{q}_\alpha(t) + \frac{\omega_\alpha}{Q_\alpha} \dot{q}_\alpha(t) + \omega_\alpha^2 q_\alpha(t) = \frac{f_\alpha(t)}{M} \quad (37)$$

where an empirical damping term, proportional to the system velocity, has been added; $f_\alpha(t)$ is the generalized force, given by

$$f_\alpha(t) = \int_{Vol} \vec{f}(\vec{r}, t) \cdot \vec{\xi}_\alpha(\vec{r}) dV \quad (38)$$

The solution of equation (37), satisfying the initial conditions (33), can be written in term of a Green function integral as [13]:

$$q_\alpha(t) = \frac{1}{M\omega_\alpha} \int_0^t f_\alpha(t') \sin \omega_\alpha(t - t') \exp -\frac{t - t'}{\tau_\alpha} dt' \quad (39)$$

⁴ In this section we shall label with greek indices the *mechanical* normal modes of the system, and with latin indices the normal modes of the *electromagnetic field* stored inside the system.

with $\tau_\alpha = 2Q_\alpha/\omega_\alpha$ is the amplitude decay time of the system.

In the frequency domain the asymptotic solution of equation (37) is easily found to be:

$$q_\alpha(\omega) = \frac{f_\alpha(\omega)/M}{\omega_\alpha^2 - \omega^2 + j\omega\omega_\alpha/Q_\alpha} \quad (40)$$

Substituting into eq. (34), we find

$$\vec{u}(\vec{r}, \omega) = \sum_{\alpha=1}^{\infty} \frac{f_\alpha(\omega)\vec{\xi}_\alpha(\vec{r})/M}{\omega_\alpha^2 - \omega^2 + j\omega\omega_\alpha/Q_\alpha} \quad (41)$$

It is clear from eq. (41), that if we are interested in the displacement in a narrow frequency interval $\omega \pm \delta\omega$, only those modes for which $\omega_\alpha \approx \omega$ (and $f_\alpha \neq 0$), will give a significant contribution.

A. Interaction of a g.w. with the mechanical structure of the detector

An incoming gravitational wave manifests itself as a tidal force density acting on the mechanical structure of the detector. Given the expression of the gravitational force and the mechanical properties of the detector, the resulting deformation can be calculated, with the aid of the mathematical apparatus outlined in the previous section.

We are mainly interested in the evaluation of the coupling coefficient $C_{ij}(t)$. Let us note that, for small displacements, we can write the integral over the perturbed volume as a surface integral in the form (see fig. 1):

$$C_{ij}(t) = \int_V (\vec{H}_i \cdot \vec{H}_j - \vec{E}_i \cdot \vec{E}_j) dV \approx \int_S (\vec{H}_i \cdot \vec{H}_j - \vec{E}_i \cdot \vec{E}_j) \vec{u}(t) \cdot d\vec{S} \quad (42)$$

where the integral in the r.h.s of eq. (42) is now performed over the *unperturbed* detector boundary. It is worth noting that this integral can be expressed as a superposition of the mechanical normal modes of the system. Using the expansion theorem (34) we can write:

$$C_{ij}(t) = \int_S (\vec{H}_i \cdot \vec{H}_j - \vec{E}_i \cdot \vec{E}_j) \vec{u}(t) \cdot d\vec{S} = \sum_{\alpha=1}^{\infty} q_\alpha(t) \int_S (\vec{H}_i \cdot \vec{H}_j - \vec{E}_i \cdot \vec{E}_j) \vec{\xi}_\alpha \cdot d\vec{S} = \sum_{\alpha=1}^{\infty} q_\alpha(t) C_{ij}^\alpha \quad (43)$$

where we have defined the time-independent form factor C_{ij}^α as:⁵

$$C_{ij}^\alpha = \int_S (\vec{H}_i \cdot \vec{H}_j - \vec{E}_i \cdot \vec{E}_j) \vec{\xi}_\alpha \cdot d\vec{S} \quad (44)$$

If the external force couples strongly only to one mechanical mode of the detector (say the m), we can write the simplified expression

$$C_{ij}(t) = q_m(t) C_{ij}^m \quad (45)$$

⁵ We remind that the superscript α labels the *mechanical* normal mode, while the subscripts i and j label the *electromagnetic* modes.

In summary, to have an effective coupling between the two electromagnetic modes we need:

1. that the generalized coordinate $q_m(t)$ is different from zero. If the system is initially at rest, this is true if and only if the generalized force, is itself different from zero, as is shown in eqs. (37) and (39);
2. that the spatial integral in eq. (44) is different from zero. In section VI we shall discuss how this depends on the symmetries of the electromagnetic field *and* of the perturbed volume.

IV. DETECTOR DESIGN

In order to build a realistic detector a suitable cavity shape has to be chosen. From quite general arguments a detector based on two coupled spherical cavities looks very promising (see fig. 2).

In order to approach the interesting frequency range for g.w. detection, the mode splitting (i.e. the detection frequency) will be $\omega_2 - \omega_1 \approx 10$ kHz. The internal radius of the spherical cavity will be $r \approx 100$ mm, corresponding to a frequency of the TE_{011} mode $\omega \approx 2$ GHz. The overall system mass and length will be $M \approx 5$ kg and $L \approx 0.8$ m. The choice of these frequencies for the resonator and mode splitting will be also useful in order to test the feasibility of a detector working at ≈ 200 MHz and at a detection frequency of ≈ 1 KHz.

A tuning cell, or a superconducting bellow, will be inserted in the coupling tube between the two cavities, allowing to tune the coupling strength (i.e. the detection frequency) in a narrow range around the design value.

From the point of view of the electromagnetic design the spherical cell has the highest geometrical factor, and so the highest quality factor, for a given surface resistance. For the TE_{011} mode of a sphere the geometric factor G has a value $G \approx 850 \Omega$, while for a standard elliptical accelerating cavity the TM_{010} mode has a value of $G \approx 250 \Omega$. Looking at the best reported values of quality factor of accelerating cavities, which typically are in the range 10^{10} – 10^{11} , we can extrapolate that the quality factor of the TE_{011} mode of a spherical cavity can exceed $Q \approx 10^{11}$.

From the mechanical point of view it is well known that a sphere has the highest interaction cross-section with a g.w. and that only a few mechanical modes of the sphere do interact with a gravitational perturbation (the quadrupolar ones) [11]. The mechanical design is highly simplified if the spherical geometry is used since the deformation of the sphere is given by the superposition of just one or two normal modes of vibration and thus can be easily modeled. In fact the proposed detector acts essentially as a standard g.w. resonant bar detector: the gravitational perturbation interacts with the mechanical structure of the resonator, deforming it. The e.m. field stored inside the resonator is affected by the time-varying boundary conditions and a small quantity of energy is transferred from the initially excited e.m. mode to the initially empty one, provided the g.w. frequency equals the frequency difference of the two modes. We emphasize that our detector is sensitive to the polarization of the incoming gravitational signal: once the e.m. axis has been chosen inside the resonator, a g.w. with polarization axes in the direction of the field axis will drive the energy transfer between the two modes of the cavity with maximum efficiency.

Finally the spherical cells can be easily deformed in order to remove the unwanted e.m. modes degeneracy and to induce the field polarization suitable for g.w. detection. The

interaction between the stored e.m. field and the time-varying boundary conditions is not trivial and depends both on how the boundary is deformed by the external perturbation and on the spatial distribution of the fields inside the resonator, as shown by the expression of the coupling coefficient C_{21}^m (eq. (44)). It has been calculated that the optimal field spatial distribution is with the field axis of the two cavities orthogonal to each other (see fig. 3). Different spatial distributions (e.g. with the field axis along the resonators' axis) give a smaller effect or no effect at all. A more detailed discussion of the coupling coefficient calculation is done in section VI.

V. FIELD EQUATIONS

We shall derive the equations of motion for the fields in the coupled system from a general hamiltonian formalism [14]. The hamiltonian of the electromagnetic field inside a resonator with perfectly conducting walls can be written, in terms of the fields amplitudes:

$$H = \frac{1}{2} \int_V (\epsilon_0 \vec{E} \cdot \vec{E} + \mu_0 \vec{H} \cdot \vec{H}) dV \quad (46)$$

If we substitute eqs. (7)–(8) in eq. (46) and use the orthonormality condition, the hamiltonian for the field becomes:

$$H = \frac{1}{2} \sum_n (\mathcal{E}_n^2 + \mathcal{H}_n^2) \quad (47)$$

If we define a generalized coordinate X_n as:

$$X_n = \frac{\mathcal{H}_n}{\omega_n} \quad (48)$$

and its conjugate momentum as:

$$P_n = \mathcal{E}_n \quad (49)$$

the hamiltonian can be written as:

$$H = \frac{1}{2} \sum_n (P_n^2 + \omega_n^2 X_n^2) \quad (50)$$

which is identical to the hamiltonian of an infinite set of uncoupled harmonic oscillators. It can be easily verified that the field equations of motion can be derived from this hamiltonian by:

$$\begin{aligned} \frac{\partial H}{\partial X_n} &= -\dot{P}_n = \omega_n^2 X_n \\ \frac{\partial H}{\partial P_n} &= \dot{X}_n = P_n \end{aligned} \quad (51)$$

which, in terms of the fields become:

$$\begin{aligned} \frac{d\mathcal{E}_n}{dt} &= -\omega_n \mathcal{H}_n \\ \frac{d\mathcal{H}_n}{dt} &= \omega_n \mathcal{E}_n \end{aligned} \quad (52)$$

which are identical to eqs. (15)–(16) if wall dissipation is neglected.

A. Field equations for the perturbed system

In order to find the equations of motions for the fields in the perturbed resonator we shall make use of the results obtained in the previous sections. Let us consider again an external time-dependent perturbation, whose rate of change is much less than the rate of change of the fields. The normal modes in the perturbed resonator are given by eqs. (19)–(31). If we are looking for the fields in a frequency region where only two electromagnetic modes give a significant contribution, the hamiltonian of the system, as a function of the *perturbed* modes amplitudes (see eqs. (22) and (23), will be:

$$H = \frac{1}{2} \left(\tilde{\mathcal{E}}_1^2 + \tilde{\mathcal{H}}_1^2 + \tilde{\mathcal{E}}_2^2 + \tilde{\mathcal{H}}_2^2 \right) \quad (53)$$

If we now substitute in the above expression the expansions (19) we obtain the hamiltonian written in terms of the *unperturbed* modes amplitudes:

$$H = \frac{1}{2} \left(\mathcal{E}_1^2 + \mathcal{H}_1^2 + \mathcal{E}_2^2 + \mathcal{H}_2^2 + \frac{p_m^2}{M} + M\omega_m^2 q_m^2 \right) + \frac{q_m}{2} \left(C_{11}^m \mathcal{H}_1^2 + C_{22}^m \mathcal{H}_2^2 + 2 C_{12}^m \mathcal{H}_1 \mathcal{H}_2 \right) - q_m f_m \quad (54)$$

where the hamiltonian of a mechanical harmonic oscillator, coupled to an external, time-dependent force, has been included.

From this hamiltonian the equations of motion for the fields can readily be obtained:

$$\frac{d\mathcal{H}_1}{dt} - \omega_1 \mathcal{E}_1 = -\frac{\omega_1}{Q_1} \mathcal{H}_1 \quad (55)$$

$$\frac{d\mathcal{H}_2}{dt} - \omega_2 \mathcal{E}_2 = -\frac{\omega_2}{Q_2} \mathcal{H}_2 \quad (56)$$

$$\frac{d\mathcal{E}_1}{dt} + \omega_1 \mathcal{H}_1 = -\omega_1 q_m (C_{11}^m \mathcal{H}_1 + C_{12}^m \mathcal{H}_2) \quad (57)$$

$$\frac{d\mathcal{E}_2}{dt} + \omega_2 \mathcal{H}_2 = -\omega_2 q_m (C_{12}^m \mathcal{H}_1 + C_{22}^m \mathcal{H}_2) \quad (58)$$

$$\frac{dq_m}{dt} - \frac{p_m}{M} = -\frac{\omega_m}{Q_m} q_m \quad (59)$$

$$\frac{dp_m}{dt} + M\omega_m^2 q_m = f_m - f_m^{ba} \quad (60)$$

where the dissipative terms have been added *by hand* and where the term f_m^{ba} , which describes the back-action effect of the fields on the walls is given by:

$$f_m^{ba} = \frac{1}{2} \left(C_{11}^m \mathcal{H}_1^2 + C_{22}^m \mathcal{H}_2^2 \right) + C_{12} \mathcal{H}_1 \mathcal{H}_2 \quad (61)$$

VI. COUPLING COEFFICIENT CALCULATION

The explicit calculation of the coupling coefficient C_{21}^m is not trivial for an arbitrary deformation of the resonator volume and in general can be done only by numerical methods.

First let us note a general property of the coupling coefficients. Let us consider the resonant modes of the two coupled cavities. As previously noted we have the symmetric and the antisymmetric mode; for the former the electric field \vec{E} and the magnetic field \vec{H} in the first cavity are equal to the electric and magnetic field in the second cavity, while for the latter \vec{E} and \vec{H} in the first cavity are equal respectively to $-\vec{E}$ and $-\vec{H}$ in the second one. From this it follows that in the definition of C_{21} , the integrand expression $(\vec{H}_2 \cdot \vec{H}_1 - \vec{E}_2 \cdot \vec{E}_1)$ – where we remind that the subscript 1 indicates the symmetric mode and 2 the antisymmetric mode – is *odd* over the whole detector volume. For this reason if the volume perturbation, over which we perform the integration, is symmetric between the two cavities, the coupling coefficient vanishes, because the contributions to the integral coming from the two cavities, cancel each other. Otherwise, if the volume perturbation is antisymmetric (when one cavity shrinks, the other expands) the two contributions are added with the same sign, and the coupling coefficient is maximum. This general property suggests that we must find a geometrical configuration of our detector such that the volume deformation due to a g.w. is antisymmetric for the two cavities. This was pointed out already in previous works, where the argument was based on the fact that, since the g.w. carries an angular momentum equal to 2, the angular momenta of the fields of the two modes should differ by 2. This can be achieved by putting the two cavities at right angle or by a suitable polarization of the electromagnetic field inside the resonator.

These concepts were verified by both analytical and numerical calculations. General arguments suggested that for an ideal spherical hollow resonator, excited in the fundamental quadrupolar mechanical mode and in the TE₀₁₁ electromagnetic mode, we should have⁶:

$$\begin{aligned}
 C_{21}^m = C_{12}^m &= \int_S (\vec{H}_1 \cdot \vec{H}_2) \vec{\xi}_m \cdot d\vec{S} = 0.4 \\
 C_{11}^m &= \int_S (\vec{H}_1 \cdot \vec{H}_1) \vec{\xi}_m \cdot d\vec{S} = 0 \\
 C_{22}^m &= \int_S (\vec{H}_2 \cdot \vec{H}_2) \vec{\xi}_m \cdot d\vec{S} = 0
 \end{aligned}
 \tag{62}$$

More detailed calculations, made on a realistic model of the coupled spheres, including the central coupling cell and the e.m. input and output ports, were made by finite element methods. These calculations showed that $C_{11}^m = C_{11}^m \leq 10^{-4}$, while $C_{12}^m = C_{21}^m \approx 0.2$.

VII. CALCULATION OF THE DETECTOR'S SIGNAL

As already pointed out in the introduction, the proposed detector exploits the energy transfer induced by the gravitational wave between two levels of an electromagnetic resonator, whose frequencies ω_1 and ω_2 are both much larger than the angular frequency Ω of the g.w. and satisfy the resonance condition $\omega_2 - \omega_1 \approx \Omega$. This is an example of a frequency

⁶ We remind that for a TE e.m. mode we have vanishing electric field on the resonator's surface; for this reason the electric field plays no role in the coupling coefficient calculation.

converter, i.e. a nonlinear device in which energy is transferred from a reference frequency to a different frequency by an external pump signal. This can be viewed as a three-bodies interaction (given by the field–wall interaction term in the hamiltonian (54)) which corresponds to annihilation of quanta at ω_1 and ω_m and creation at ω_2 (or vice versa). For this reason we could argue that, since for a small perturbation $\mathcal{H}_1(t)$ and $\mathcal{E}_1(t)$ will approximately be sinusoidal functions at frequency ω_1 , while $\mathcal{H}_2(t)$ and $\mathcal{E}_2(t)$ will oscillate at frequency ω_2 , in the hamiltonian only the terms varying as $\omega_2 - \omega_1$ will give a significant contribution to the interaction. The d–c terms will just give an average deformation of the detector’s walls, determining a static frequency shift of the resonant modes, while the rapidly fluctuating terms at $\omega_2 + \omega_1$ would practically average to zero.

We shall now calculate the field that is excited by the boundary perturbation in mode 2, starting from an initial condition with mode 1 strongly excited in the resonator. To simplify the analysis of the system of differential equations (55)–(60) we will neglect the small perturbation, due to the external force, on the initially excited e.m. mode (mode 1), and will set $\mathcal{H}_1 \approx A_1 \cos(\omega_1 t)$ and $\mathcal{E}_1 \approx A_1 \sin(\omega_1 t)$, with *constant* amplitude A_1 .⁷ Furthermore we shall consider the coupling between two TE modes of a resonator: for these modes we have vanishing electric field on the resonator surface. Switching to the complex notation,⁸ we obtain:

$$f_m^{ba} \approx \frac{1}{2} C_{21}^m \Re(\mathcal{H}_2 \mathcal{H}_1^*) \quad (63)$$

Finally, to further simplify our calculations, we shall choose a resonator geometry and e.m. field distribution so that $C_{11}^m = C_{22}^m = 0$. We shall see in a following section that this choice is always possible.

With this assumptions, and taking $\mathcal{Q}_1 \approx \mathcal{Q}_2 \equiv \mathcal{Q}$, we can recast the coupled system of equations in the following form:

$$\ddot{\mathcal{H}}_2 + \frac{\omega_2}{\mathcal{Q}} \dot{\mathcal{H}}_2 + \omega_2^2 \mathcal{H}_2 = -\omega_2^2 q_m C_{21}^m \mathcal{H}_1 \quad (64)$$

$$\ddot{q}_m + \frac{\omega_m}{Q_m} \dot{q}_m + \omega_m^2 q_m = \frac{f_m}{M} - \frac{1}{2} \frac{C_{21}^m}{M} \mathcal{H}_2 \mathcal{H}_1^* \quad (65)$$

We apply the following substitutions:

$$\begin{aligned} \mathcal{H}_2(t) &= A_2(t) \exp(i \omega_2 t) \\ q_m(t) &= Q(t) \exp(i \Omega t) \\ f_m(t) &= F(t) \exp(i \Omega t) \end{aligned} \quad (66)$$

Eqs. (64)–(65) now become:

$$\begin{aligned} \ddot{A}_2 + a \dot{A}_2 + b A_2 &= c Q \\ \ddot{Q} + d \dot{Q} + e Q &= g A_2 + F/M \end{aligned} \quad (67)$$

where a, b, c, d, e and g are constant coefficients defined by

$$a = 2i (\omega_1 + \Omega) + \frac{\omega_2}{\mathcal{Q}}$$

⁷ Actually the amplitude of mode 1 is kept constant by an external rf power source.

⁸ In the following it is understood that the physical fields are the real parts of the complex quantities.

$$\begin{aligned}
b &= \omega_2^2 - (\omega_1 + \Omega)^2 + i \frac{\omega_2}{Q} (\omega_1 + \Omega) \\
c &= -\omega_2^2 C_{21}^m A_1 \\
d &= 2i \Omega + \frac{\omega_m}{Q_m}
\end{aligned} \tag{68}$$

$$\begin{aligned}
e &= \omega_m^2 - \Omega^2 + i \frac{\omega_m \Omega}{Q_m} \\
g &= -\frac{1}{2} \frac{C_{21}^m A_1}{M}
\end{aligned} \tag{69}$$

We can now fourier transform eqs. (67) and solve them for $A_2(\omega)$. We find:

$$A_2(\omega) = -2\pi \frac{c F(\omega)/M}{(b - \omega^2 + i a \omega) (e - \omega^2 + i d \omega) - g c} \tag{70}$$

$\mathcal{H}_2(t)$ is then given by:

$$\mathcal{H}_2(t) = -\exp(i \omega_2 t) \int_{-\infty}^{\infty} \frac{c F(\omega)/M \exp(i \omega t)}{(b - \omega^2 + i a \omega) (e - \omega^2 + i d \omega) - g c} d\omega \tag{71}$$

For a plane g.w travelling along the z axis the force density, in the proper reference frame attached to the detector, has the form:

$$\vec{f}(\vec{x}, t) = -\frac{1}{2} \rho(\vec{x}) [(\ddot{a}_1^1 x + \ddot{a}_2^1 y), (\ddot{a}_2^1 x - \ddot{a}_1^1 y), (0)] \tag{72}$$

where $a_j^i(t)$, is the adimensional amplitude of the wave, and $a_1^1 = -a_2^2$, $a_2^1 = a_1^2$. The generalized force, acting on the m mechanical mode, then has the form

$$\begin{aligned}
f_m &= -\frac{1}{2} \ddot{a}_1^1 \int_{Vol} ((\xi_m)_x x - (\xi_m)_y y) \rho(\vec{x}) dV - \\
&\quad \frac{1}{2} \ddot{a}_2^1 \int_{Vol} ((\xi_m)_x y + (\xi_m)_y x) \rho(\vec{x}) dV
\end{aligned} \tag{73}$$

If $a_j^i(t)$ is given by:

$$a_j^i(t) = \begin{pmatrix} h_1^1 \alpha(t) & h_2^1 \beta(t) \\ h_2^1 \beta(t) & -h_1^1 \alpha(t) \end{pmatrix} \tag{74}$$

where $\alpha(t)$ and $\beta(t)$ are sinusoidal functions of frequency $\Omega/(2\pi)$, then $\ddot{a}_j^i = -\Omega^2 a_j^i$, and if we define the effective lengths of our detector as

$$\begin{aligned}
L_+ &= \frac{1}{M} \int_{Vol} ((\xi_m)_x x - (\xi_m)_y y) \rho(\vec{x}) dV \\
L_\times &= \frac{1}{M} \int_{Vol} ((\xi_m)_x y + (\xi_m)_y x) \rho(\vec{x}) dV
\end{aligned} \tag{75}$$

we can write

$$f_m(t) = \frac{1}{2} M \Omega^2 (L_+ a_1^1 + L_\times a_2^1) \tag{76}$$

and

$$A_2(\omega) = -\frac{1}{2} \frac{c \Omega^2 (L_+ h_1^1 + L_\times h_2^1)}{be - gc} \delta(\omega - \Omega) \quad (77)$$

or, making use of eq. (68)

$$\mathcal{H}_2(t) = \frac{1}{2} \frac{\omega_2^2 C_{21}^m A_1 (L_+ h_1^1 + L_\times h_2^1) \Omega^2 \exp(i \omega_2 t)}{\left(\omega_m^2 - \Omega^2 + i \frac{\omega_m \Omega}{Q_m}\right) \left(\omega_2^2 - (\omega_1 + \Omega)^2 + i \frac{\omega_2(\omega_1 + \Omega)}{Q}\right) - \frac{(\omega_2 C_{21}^m A_1)^2}{2M}} \quad (78)$$

The electric field amplitude the initially empty mode can be readily obtained from eq. (56); the average energy stored in mode number 2 is given by: $U_2 = (1/2)|\mathcal{H}_2|^2 = (1/2)|\mathcal{E}_2|^2$.

VIII. NOISE ISSUES

A. Mechanical thermal noise

Thermal noise is one of the fundamental limits in the measurement of small displacements. In particular it is one of the dominant noise sources in resonant–mass detectors of g.w. and a major reason that such detectors operate at cryogenic temperatures. Since our detector exploits the coupling of the g.w. with the mechanical structure of the resonator, we have to carefully study the thermal noise contribution to our output signal.

We start again from eqs. (64)–(65) taking now the external force $f_m(t)$ as a stochastic force with constant power spectrum S_{ff} , given by [15]:

$$S_{ff} = \frac{4Mk_B T \omega_m}{Q_m} \quad (79)$$

Making the substitutions:

$$\begin{aligned} \mathcal{H}_2(t) &= A_2(t) \exp(i \omega_2 t) \\ q_m(t) &= Q(t) \exp(i (\omega_2 - \omega_1) t) \end{aligned} \quad (80)$$

we obtain the following equations:

$$\begin{aligned} \ddot{A}_2 + a\dot{A}_2 + bA_2 &= cQ \\ \ddot{Q} + d\dot{Q} + eQ &= gA_2 + \frac{f(t)}{M} \exp(i (\omega_1 - \omega_2) t) \end{aligned} \quad (81)$$

where a, b, c, d, e and g are defined as in eq. (68) with the parameter Ω replaced by the difference $\omega_2 - \omega_1$.

The first equation in (81) can be solved for $Q(t)$, and we are left with one equation for the variable $A_2(t)$:

$$\begin{aligned} -\frac{d^4 A_2}{dt^4} - (d + a) \frac{d^3 A_2}{dt^3} - (b + e + ad) \frac{d^2 A_2}{dt^2} - (db + ea) \frac{dA_2}{dt} + (cg - eb) A_2 = \\ c \frac{f(t)}{M} \exp(i (\omega_1 - \omega_2) t) \end{aligned} \quad (82)$$

For a linear system we can immediately write the spectral density of the amplitude A_2 as [15]:

$$S_{AA}(\omega) = |p(\omega)|^{-2} \left(\frac{c}{M} \right)^2 S_{ff} \quad (83)$$

with

$$p(\omega) = -\omega^4 + i(a+d)\omega^3 + (e+b+da)\omega^2 - i(ea+db)\omega + cg - eb \quad (84)$$

being the fourier transform of the linear system's impulse response function.

From the above equations we readily find the spectral densities of $\mathcal{H}_2(t)$ as:

$$S_{HH}(\omega) = |p(\omega - \omega_2)|^{-2} (\omega_2 C_{21}^m A_1)^2 \frac{4k_B T \omega_m}{M Q_m} \quad (85)$$

B. Other noise sources

1. Master oscillator phase noise

To operate our device we have to feed microwave power into one resonant mode (say mode 1), in order to detect the energy transfer between the full and the initially empty mode driven by the external perturbation.

To feed power into our device we shall use a voltage controlled microwave oscillator locked on mode 1, at frequency ω_1 . The master oscillator phase noise is filtered through the resonator linewidth; the power spectral density has the following frequency dependence [8]:

$$S_{LO}(\omega) = \frac{4\beta P_I / (\omega_1 Q)}{(1/Q)^2 + (\omega/\omega_1 - \omega_1/\omega)^2} \quad (86)$$

where P_I is the power input level and β is the coupling coefficient of mode 1 to the output load. From the above equation we can estimate the microwave power noise spectral density at the detection frequency ω_2 :

$$S_{LO}(\omega_2) = \frac{4\beta P_I / (\omega_1 Q)}{(1/Q)^2 + (\omega_2/\omega_1 - \omega_1/\omega_2)^2} \approx \beta \frac{P_I}{\omega_1 Q} \left(\frac{\omega_2}{\omega_2 - \omega_1} \right)^2 \quad (87)$$

This figure can be improved if the receiver discriminates the parity of the e.m. field at frequency ω_2 , i.e. if it is sensitive only to the power excited in mode number 2, rejecting all contributions coming from mode number 1. In this way mode 1 becomes decoupled from the output load and $\beta = 0$. The experimental set-up, based on the use of two magic-tees which accomplishes this issue is discussed in detail in [5]. Of course the mode discrimination cannot be ideal, and some power leaking from mode 1 to the detector's output will be present. Nevertheless our previous work has demonstrated that with a careful tuning of the detection electronics we can obtain $\beta \leq 10^{-14}$ [5].

2. Amplifier noise

The input Johnson noise of the first amplifier in the detection electronics has to be added to the previous contributions to establish the overall noise spectral density. It can be described by the frequency independent spectral density [15]:

$$S_{JJ} = k_B T \times 10^{(N/10)} \equiv k_B T_{eq} \quad (88)$$

where N is the noise figure of the amplifier (in dB) and T the operating temperature.

IX. DETECTOR SENSITIVITY

The detector sensitivity is ultimately determined by the overall effect of the various noise sources discussed in section VIII and, eventually, by several others. Of course, depending on the characteristics of the system and on the experimental set-up, different noise sources will become dominant.

We shall characterize the noise in our detector by a frequency dependent spectral density $S_n(f)$, with dimension Hz^{-1} , defined as follows [16]: if a sinusoidal g.w. with known phase ϕ , known frequency f and unknown r.m.s. amplitude $\sqrt{2}h_0$, impinges on the detector, and if we try to detect the wave by Fourier analyzing the detector output with a bandwidth Δf , then the *amplitude* signal-to-noise ratio will be:

$$\frac{S}{N} = \frac{h_0}{(S_n(f) \Delta f)^{1/2}} \quad (89)$$

We shall also define the minimum detectable wave amplitude (at 90% C.L.) for a periodic source with known frequency and phase as:

$$h_{min}(f) = 1.7 \left(\frac{S_n(f)}{F} \right)^{1/2} \quad (90)$$

with dimension $\text{Hz}^{-1/2}$. In the following calculations the average pattern function value $F = 2/5$ has been taken [17].

Let us focus our attention on the system mentioned in section IV based on two spherical niobium cavities working at $\omega_1 \approx \omega_2 \approx 2$ GHz with a stored energy in the initially excited symmetric mode of $U_1 \approx 10$ J per cell. This is a small-scale system with an effective length of 0.1 m and a typical weight of 5 kg. The lowest quadrupolar mechanical mode is at $\omega_m \approx 4$ kHz. In the following we shall consider an equivalent temperature of the detection electronics $T_{eq} = 30$ K.

A possible design of the detector uses both the mechanical resonance of the structure, and the e.m. resonance. This can be accomplished if the detector is designed in order to have the mechanical mode frequency equal to the e.m. modes frequency difference $\omega_m \approx \omega_2 - \omega_1$. In this frequency range, with reasonable values for the system parameters, the dominant noise source will be the noise coming from the brownian motion of the detector walls. The expected sensitivity of the detector for $\omega_2 - \omega_1 = \omega_m = 4$ kHz is shown in figure 4. In figure 5 the separate contribution of the noise sources – discussed in section VIII – to the overall noise spectral density is shown. We point out that even if in this case the dominant noise source is the walls thermal motion a lower T_{eq} would increase the detection bandwidth, as shown in figure 6.

Since our detector is based on a double resonant system (the mechanical resonator and the electromagnetic resonator) it can be operated also for frequencies $\omega_2 - \omega_1 \neq \omega_m$. At frequencies $\omega_2 - \omega_1 \leq 1$ kHz the master oscillator phase noise will, in general, be dominant (see sec. VIII B 1), while at frequencies $\omega_2 - \omega_1 \geq 10$ kHz the noise coming from the detection electronics will dominate (at least for $T_{eq} \approx 30$ K), as shown in figure 7. The expected sensitivity of the detector for $\omega_2 - \omega_1 = 10$ kHz is shown in figure 8.

In order to work at frequencies $\omega_2 - \omega_1 \leq 1$ kHz a large-scale system has to be developed. A possible design could be based on two spherical cavities working at $\omega_1 \approx \omega_2 \approx 500$ MHz, with $\omega_2 - \omega_1 \approx 1$ kHz. This system could have a stored energy of $U_1 \approx 800$ J per cell, an

effective length of 0.4 m and a typical weight of 300 kg. With a rather optimistic (but not unrealistic) choice of system parameters one could obtain the sensitivity shown in figure 9. We point out that in this figure an electronics equivalent temperature of $T_{eq} \approx 1$ K has been used; also in this case lowering T_{eq} corresponds to an increase of the detection bandwidth (see fig. 11).

The large-scale system could also be used at higher frequencies; in this case a good sensitivity can be achieved in a narrow detection bandwidth (see fig. 12).

X. CONCLUSIONS

A first prototype of the detector has been built and successfully tested [5]. A detector based on two coupled spherical cavities has been designed and preliminar mechanical and electromagnetic tests are being made on normal conducting prototypes. The planned timeline is as follows:

- In 2002 a bulk niobium detector (coupled spherical cavities, $\omega = 2$ GHz, $\omega_2 - \omega_1 = 10$ kHz, fixed coupling) will be built at CERN;
- In 2003 a variable coupling detector will be built and tested.

In the meantime several open problems must be addressed:

- The mechanical quality factor of the detector has to be maximized in order to suppress the noise coming from the brownian motion of the detector walls. Since mechanical dissipations arise from materials intrinsic losses and from the coupling of the system to the external environment, materials with low intrinsic losses must be used for the construction of the detector and the design of a suitable suspension system has to be done carefully.
- The requirement of an high mechanical quality factor has to be matched with the requirement of high electromagnetic quality factor. This can be accomplished by the use of bulk niobium, which, at low temperatures, has low intrinsic losses both mechanical and electromagnetic, or by the use of a niobium thin film deposited on a high mechanical quality factor substrate. Both techniques present in principle advantages and drawbacks. Several prototypes of single-cell, seamless, copper spherical cavities have been built at INFN-LNL by E. Palmieri and will be sputter-coated and tested at CERN to check the quality of niobium films deposited on spherical substrates.
- A cryogenic system with a cooling power of ≈ 5 W at $T \approx 1.8$ K and $P = 1$ bar has to be designed. The contribution of the cryogenic system to the noise has to be studied carefully.
- The readout electronics has to be optimized. The use of a low noise transducer, possibly based on the SQUID technology, has to be investigated.

If experimental results will be encouraging, by the end of 2003 a proposal for the construction of a g.w detector, based on superconducting rf cavities could be considered.

- [1] F. Pegoraro, L.A. Radicati, Ph. Bernard, and E. Picasso. Electromagnetic detector for gravitational waves. *Physics Letters*, 68A(2):165–168, 1978.
- [2] F. Pegoraro, E. Picasso, and L.A. Radicati. On the operation of a tunable electromagnetic detector for gravitational waves. *Journal of Physics A*, 11(10):1949–1962, 1978.
- [3] C.E. Reece, P.J. Reiner, and A.C. Melissinos. Observation of 4×10^{-17} cm harmonic displacement using a 10 GHz superconducting parametric converter. *Physics Letters*, 104A(6,7):341, 1984.
- [4] C.E. Reece, P.J. Reiner, and A.C. Melissinos. Parametric converters for detection of small harmonic displacements. *Nuclear Instruments and Methods*, A245:299–315, 1986.
- [5] Ph. Bernard, G. Gemme, R. Parodi, and E. Picasso. A detector of small harmonic displacements based on two coupled microwave cavities. *Review of Scientific Instruments*, 72(5):2428–2437, 2001. gr-qc/0103006.
- [6] F. Pegoraro and L.A. Radicati. Dielectric tensor and magnetic permeability in the weak field approximation of general relativity. *Journal of Physics A*, 13:2411–2421, 1980.
- [7] C.M. Caves. Microwave cavity gravitational radiation detectors. *Physics Letters*, 80B(3):323–326, 1979.
- [8] J.C. Slater. *Microwave Electronics*. D. Van Nostrand Company, Inc., New York, 1950.
- [9] G. Goubau. *Electromagnetic waveguides and cavities*. Pergamon Press, Oxford, 1961.
- [10] L.D. Landau and E.M. Lifshitz. *Theory of elasticity*. Pergamon, 1970.
- [11] J.A. Lobo. What can we learn about gw physics with an elastic spherical antenna? *Physical Review D*, 52:591, 1995.
- [12] P.R. Saulson. Thermal noise in mechanical experiments. *Physical Review D*, 42(8):2437–2445, 1990.
- [13] R. Courant and D. Hilbert. *Methods of mathematical physics*. John Wiley & Sons, New York, 1989.
- [14] W.H. Louisell. *Radiation and noise in quantum electronics*. McGraw–Hill, New York, 1964.
- [15] A. Papoulis. *Probability, Random Variables and Stochastic Processes*. McGraw–Hill, New York, 1965.
- [16] K.S. Thorne. Gravitational radiation. In S.W. Hawking and W. Israel, editors, *300 Years of Gravitation*. Cambridge University Press, Cambridge, 1987.
- [17] M. Maggiore. Gravitational wave experiments and early universe cosmology. *Physics Reports*, 331(6):283–367, 2000. gr-qc/9803028.

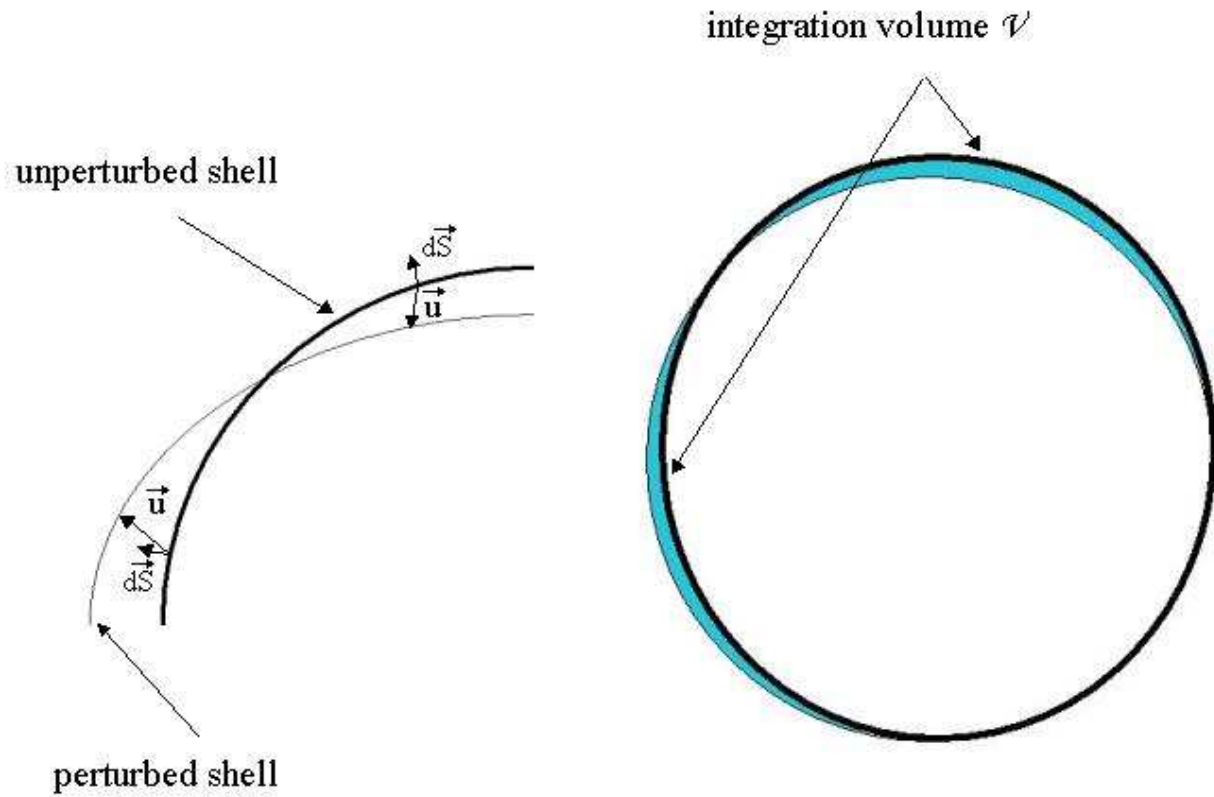


FIG. 1: Schematic view of the deformed boundary. \vec{u} is the local displacement vector; $d\vec{S}$ is a vector pointing in the direction of the *outer* normal of the original surface.

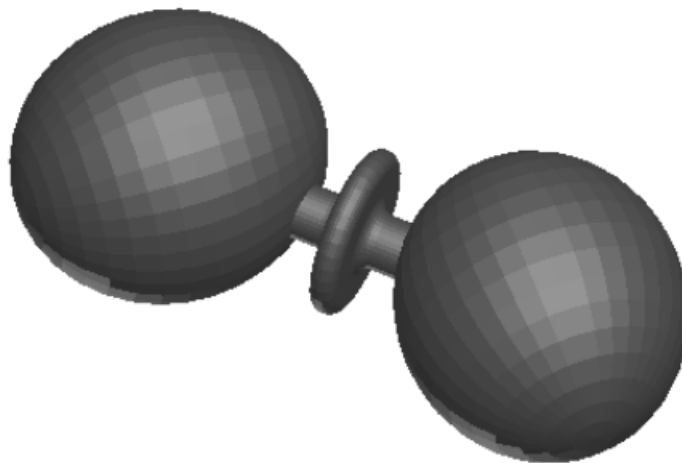


FIG. 2: Artistic view of the coupled spherical cavities with the central tuning cell.

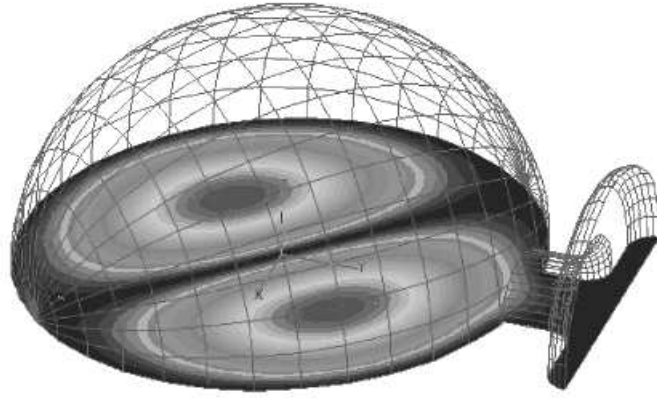


FIG. 3: Electric field magnitude of the TE_{011} mode. Note the alignment of the field axis.

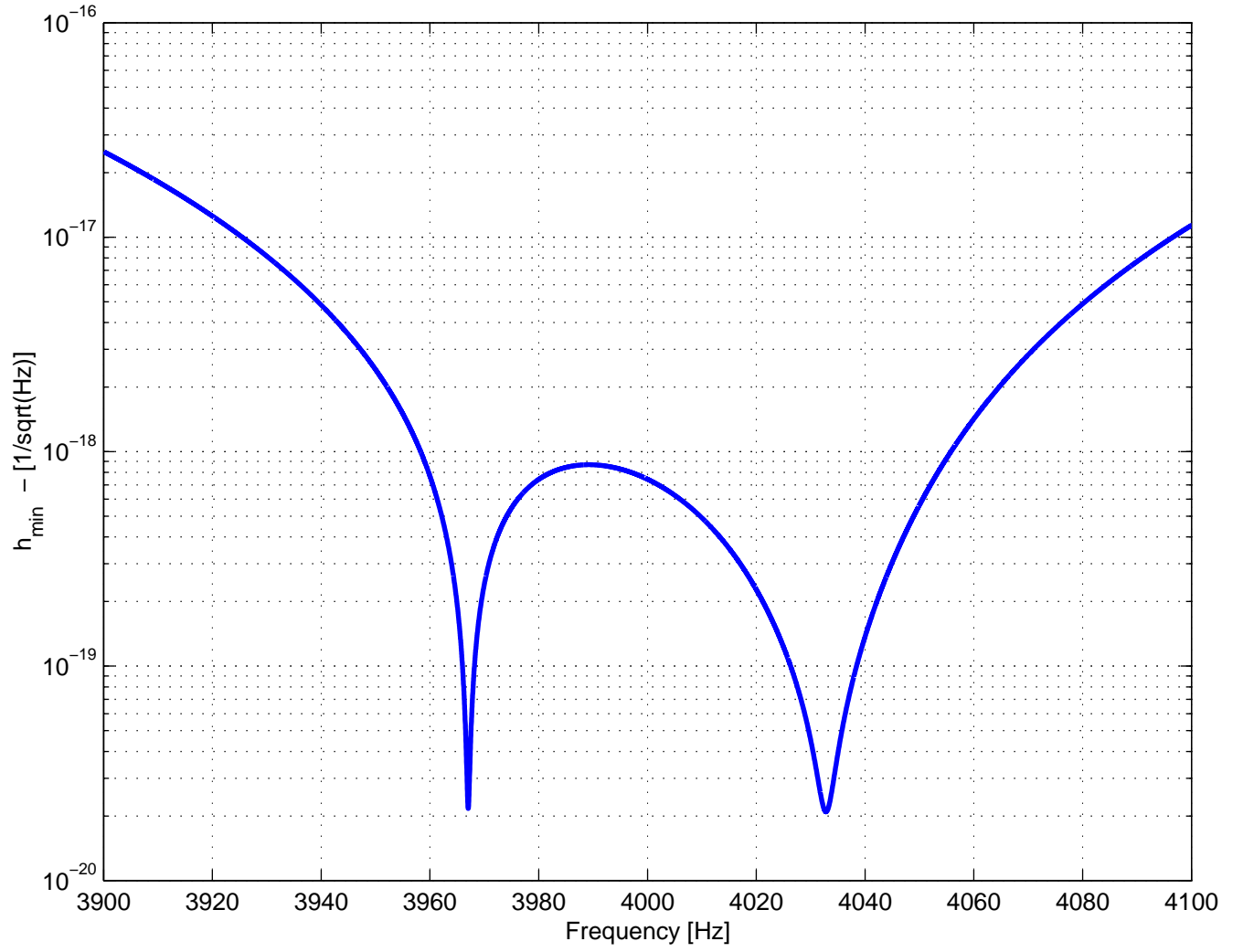


FIG. 4: Calculated small-scale system sensitivity for a periodic source ($\omega_m \approx \omega_2 - \omega_1 = 4$ kHz, $Q = 10^{10}$, $Q_m = 10^6$, $T = 1.8$ K, $T_{eq} = 30$ K).

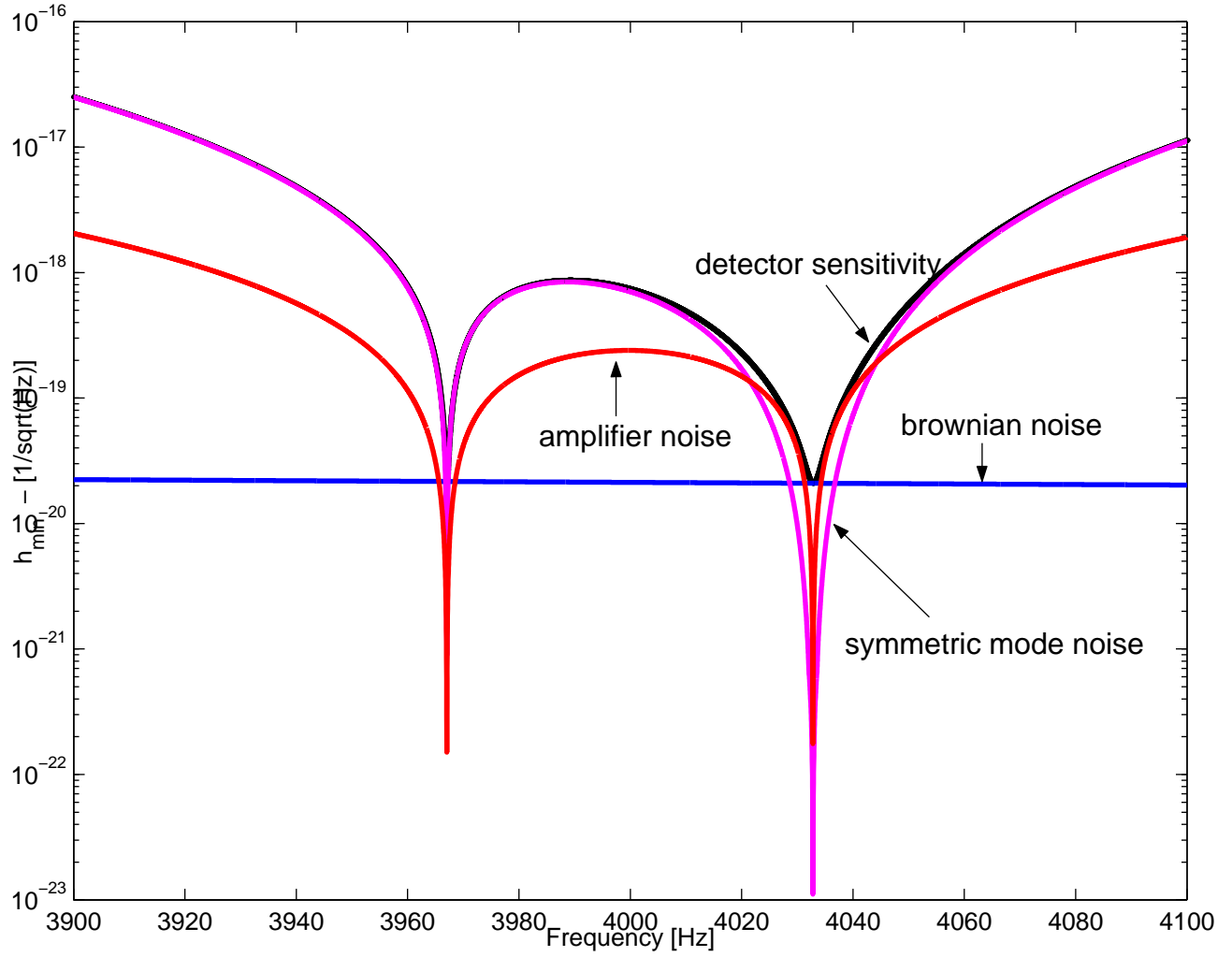


FIG. 5: Separate contribution of various noise sources to small-scale system sensitivity ($\omega_m \approx \omega_2 - \omega_1 = 4$ kHz, $Q = 10^{10}$, $Q_m = 10^6$, $T = 1.8$ K, $T_{eq} = 30$ K). As can be seen in this case the sensitivity is determined by the brownian motion of the walls while the detection bandwidth is limited by the amplifier noise.

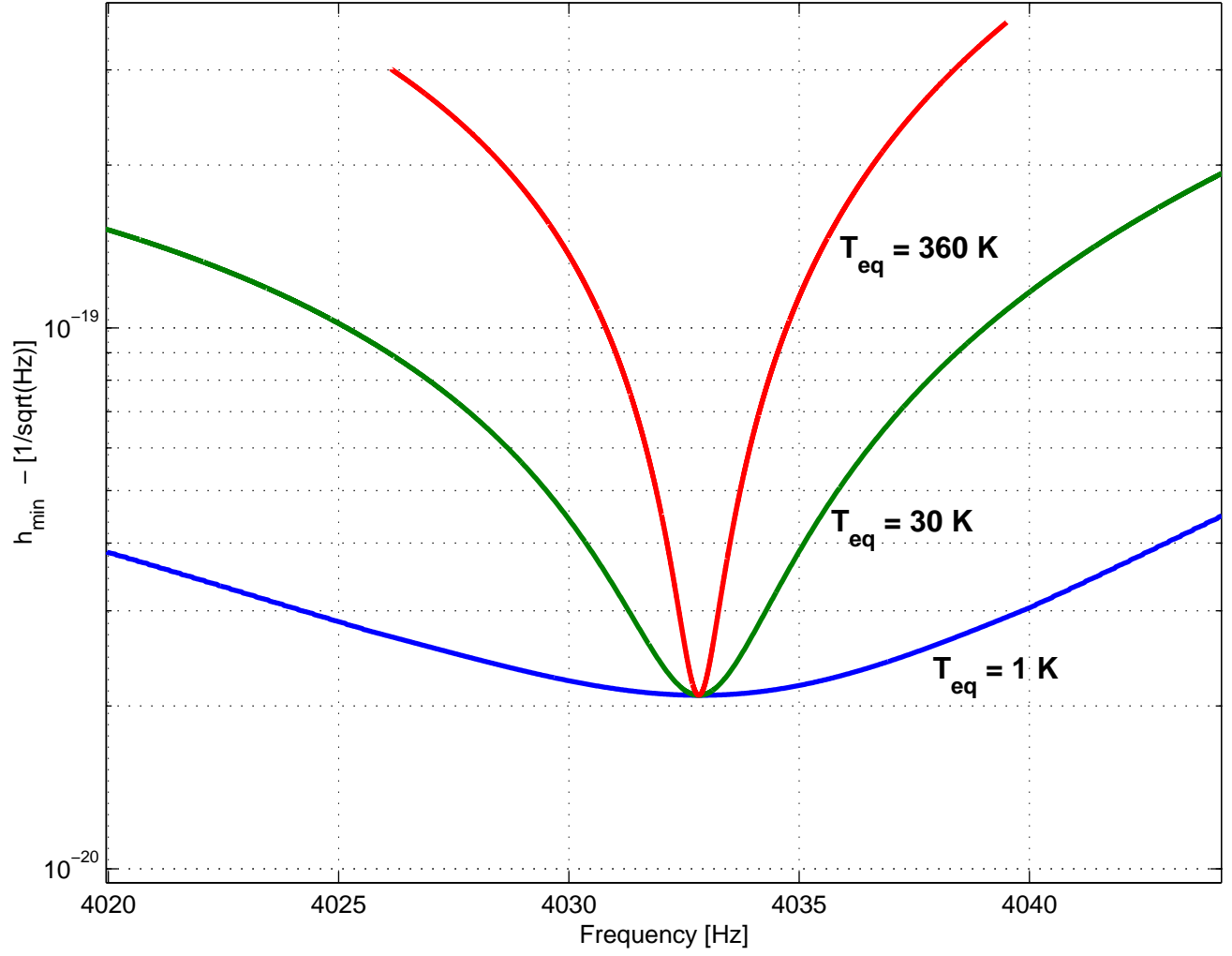


FIG. 6: Detection bandwidth vs. T_{eq} for small-scale system ($\omega_2 - \omega_1 = 4 \text{ kHz}$, $Q = 10^{10}$, $Q_m = 10^6$, $T = 1.8 \text{ K}$).

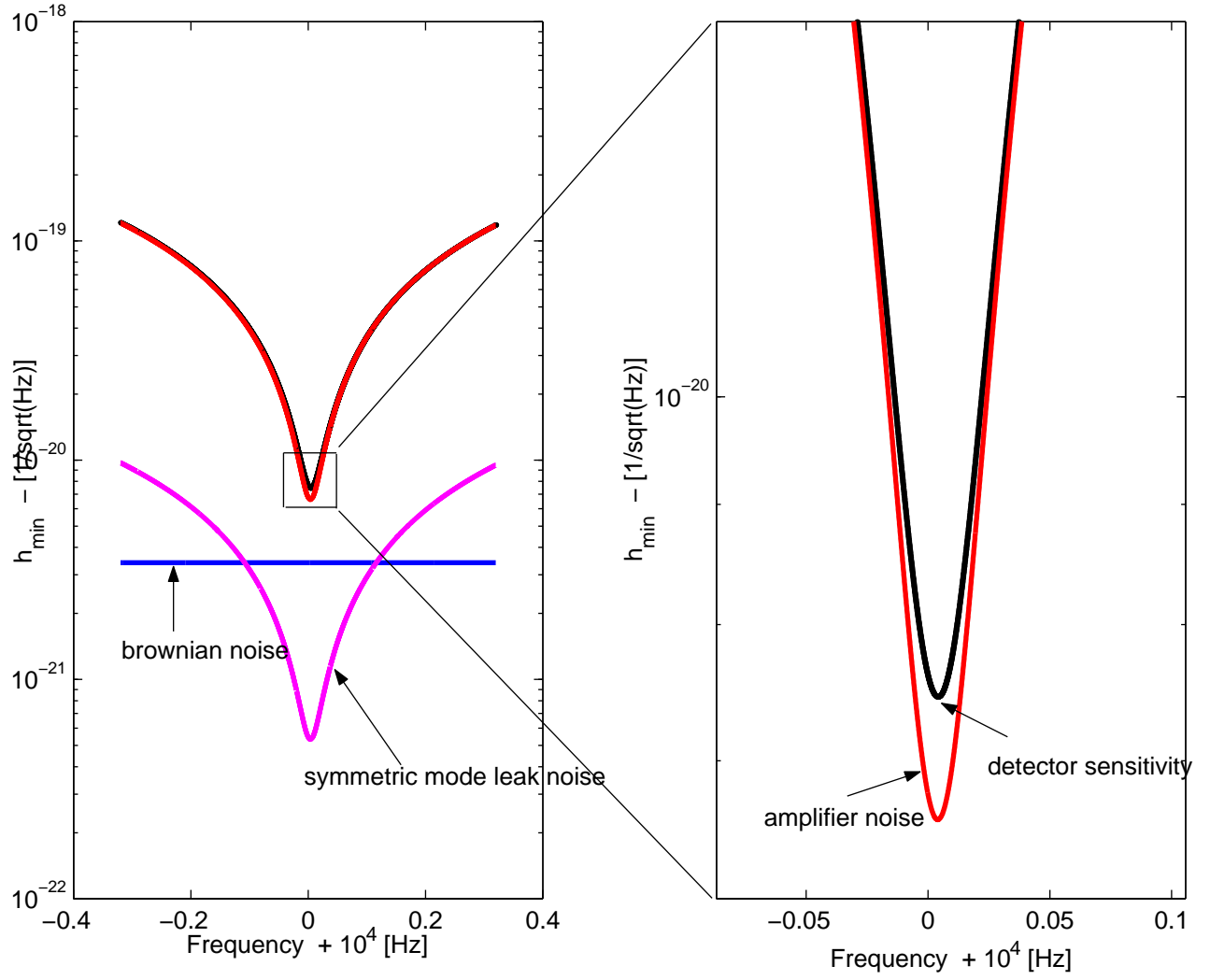


FIG. 7: Separate contribution of various noise sources to small-scale system sensitivity ($\omega_m = 4$ kHz, $\omega_2 - \omega_1 = 10$ kHz, $Q = 10^{10}$, $Q_m = 10^6$, $T = 1.8$ K, $T_{eq} = 30$ K). As can readily be seen in this case the both the sensitivity and the detection bandwidth are limited by the amplifier noise.

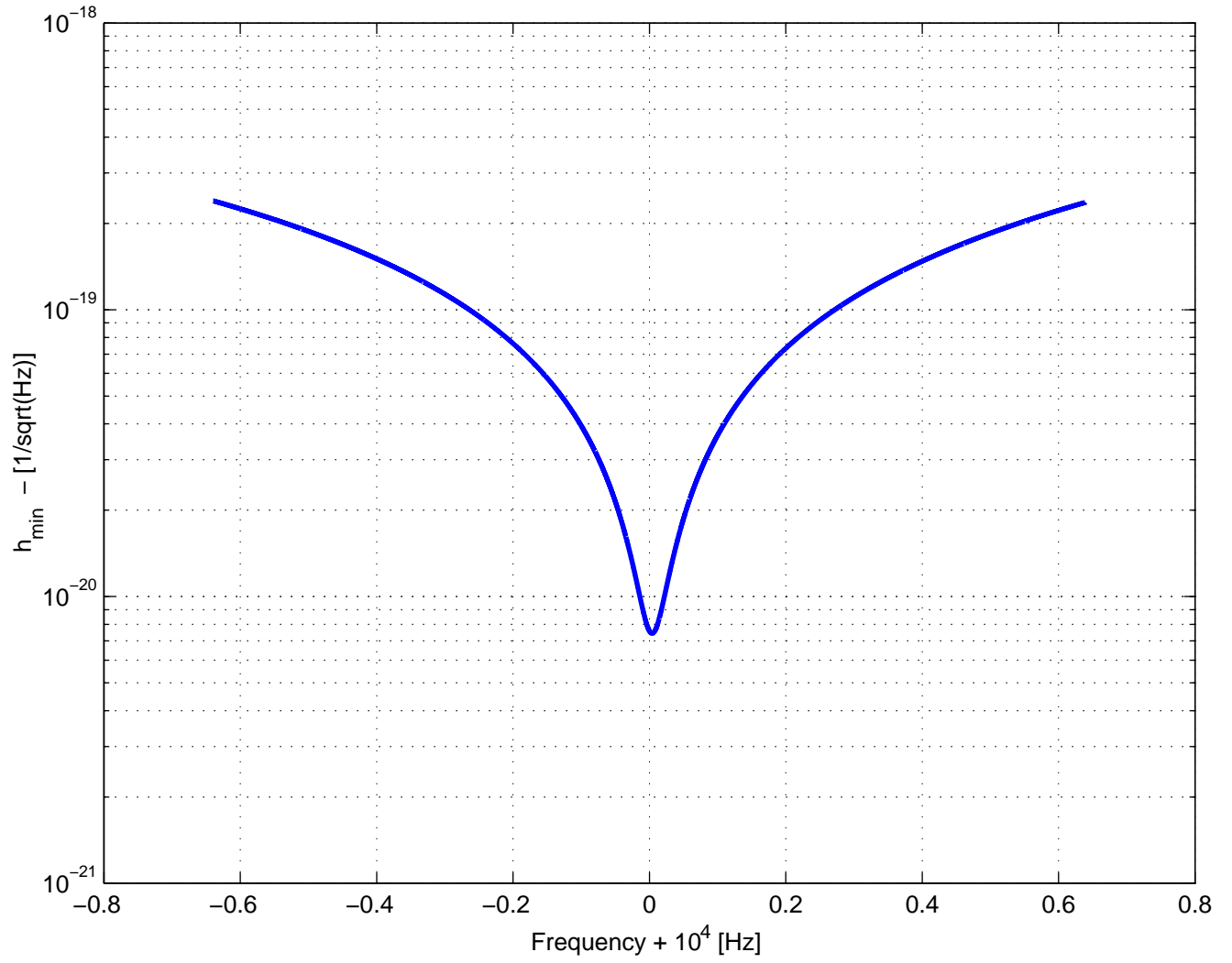


FIG. 8: Calculated small-scale system sensitivity for a periodic source ($\omega_m = 4$ kHz, $\omega_2 - \omega_1 = 10$ kHz, $Q = 10^{10}$, $Q_m = 10^6$, $T = 1.8$ K, $T_{eq} = 30$ K).

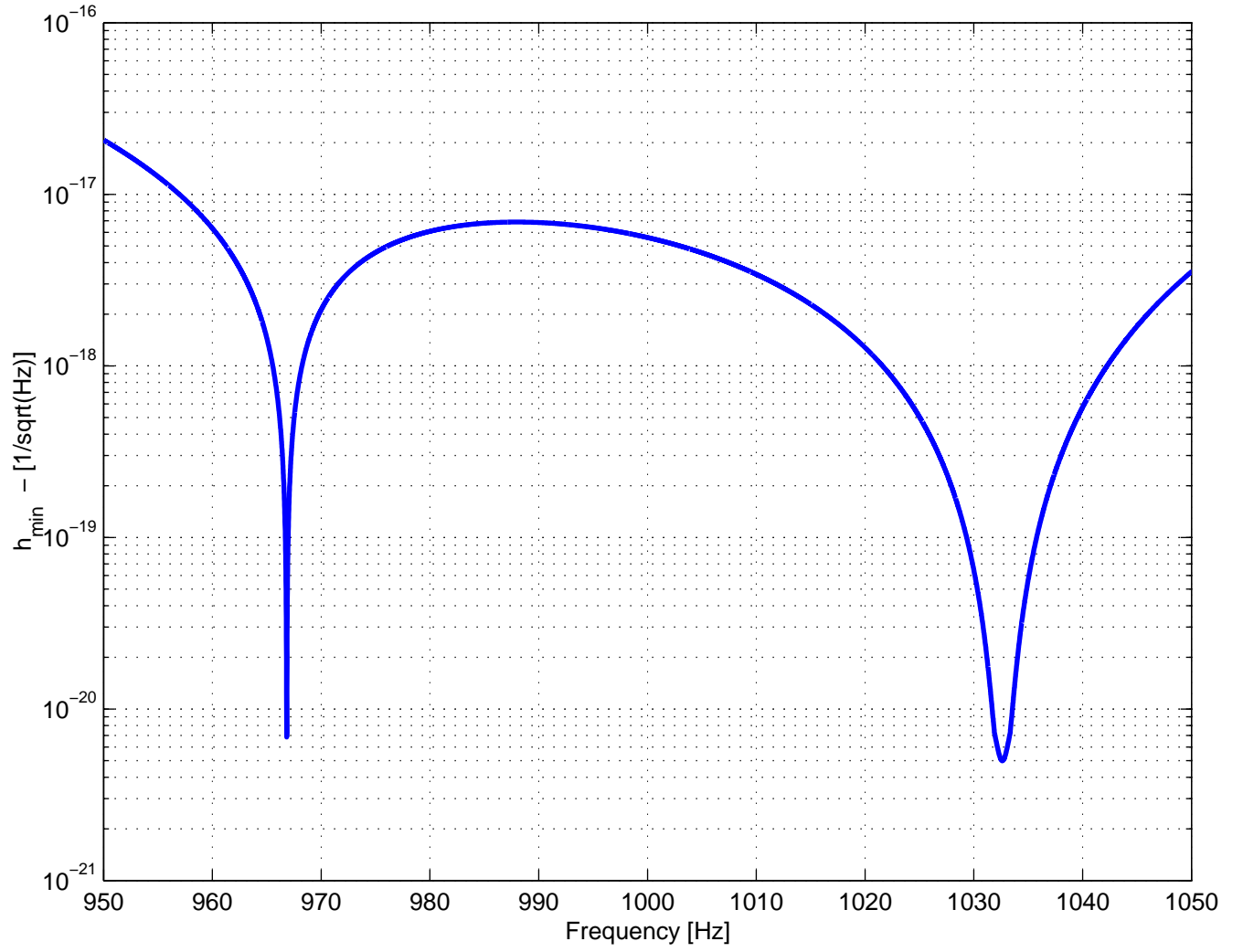


FIG. 9: Calculated large-scale system sensitivity for a periodic source ($\omega_m \approx \omega_2 - \omega_1 \approx 1$ kHz, $Q = 10^{10}$, $Q_m = 10^6$, $T = 1.8$ K, $T_{eq} = 1$ K).

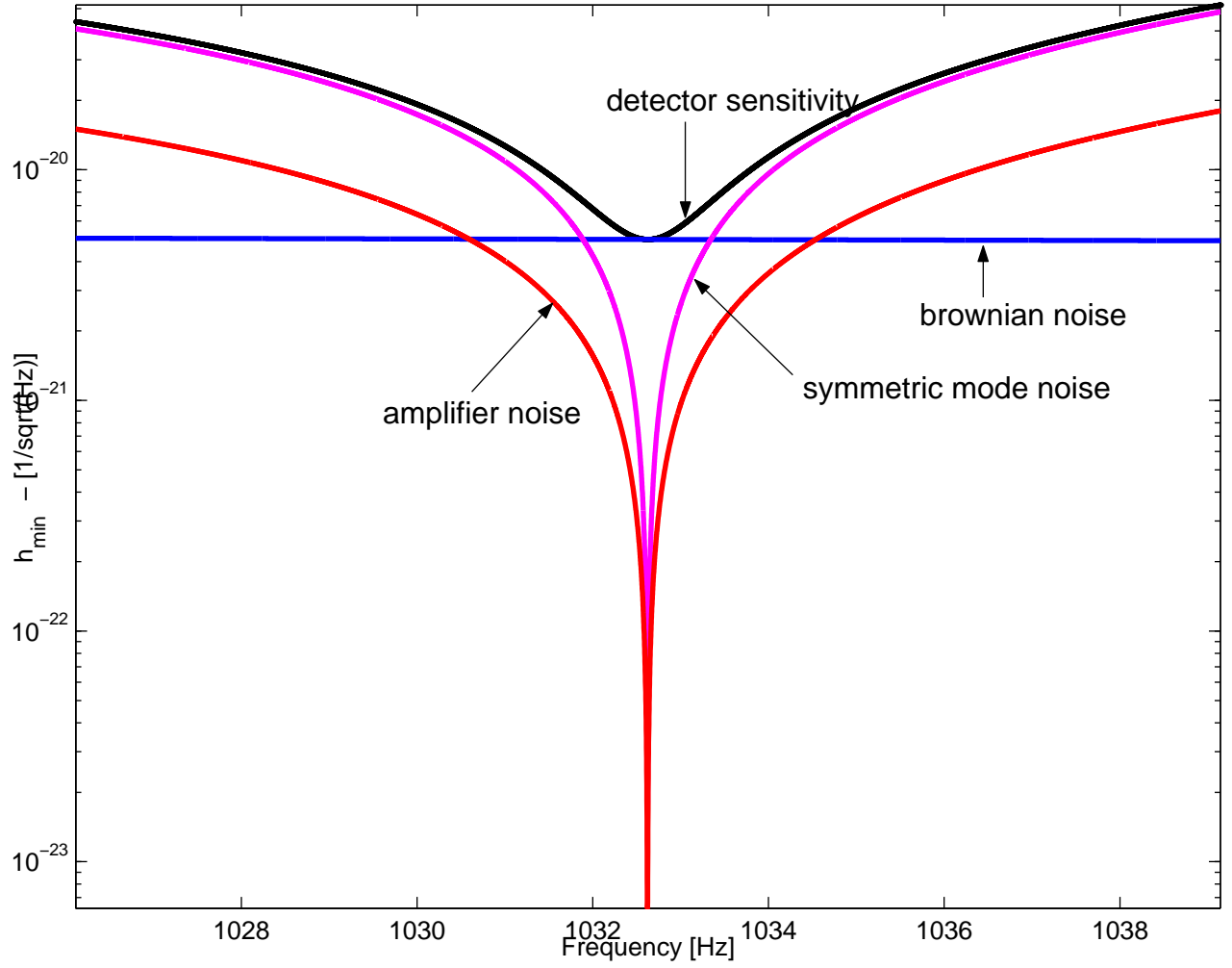


FIG. 10: Separate contribution of various noise sources to large-scale system sensitivity ($\omega_m \approx \omega_2 - \omega_1 \approx 1$ kHz, $Q = 10^{10}$, $Q_m = 10^6$, $T = 1.8$ K, $T_{eq} = 1$ K). Note that here the sensitivity is limited by the brownian noise while the detection bandwidth is set by the master oscillator phase noise.

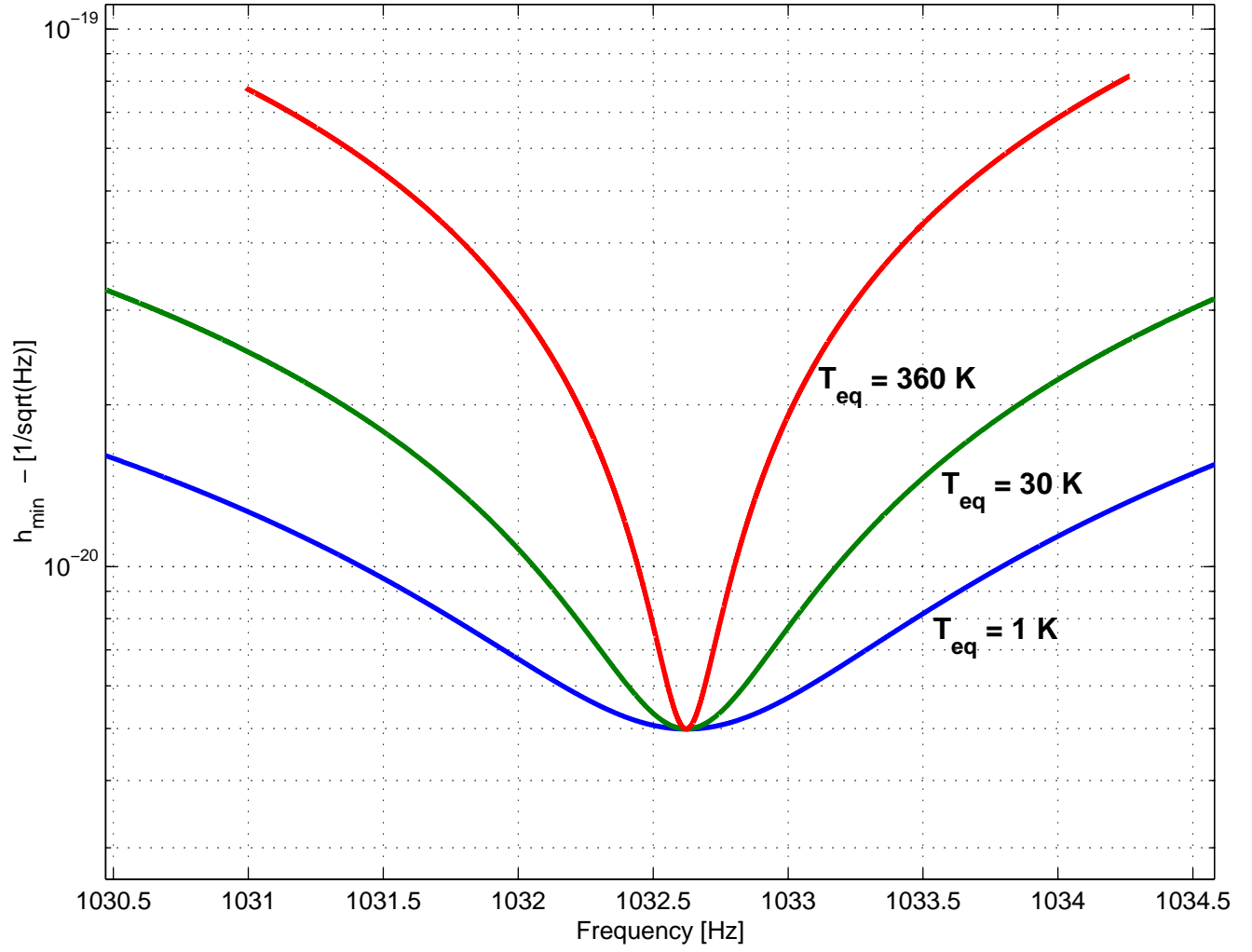


FIG. 11: Detection bandwidth vs. T_{eq} for large-scale system ($\omega_m \approx \omega_2 - \omega_1 \approx 1 \text{ kHz}$, $Q = 10^{10}$, $Q_m = 10^6$, $T = 1.8 \text{ K}$).

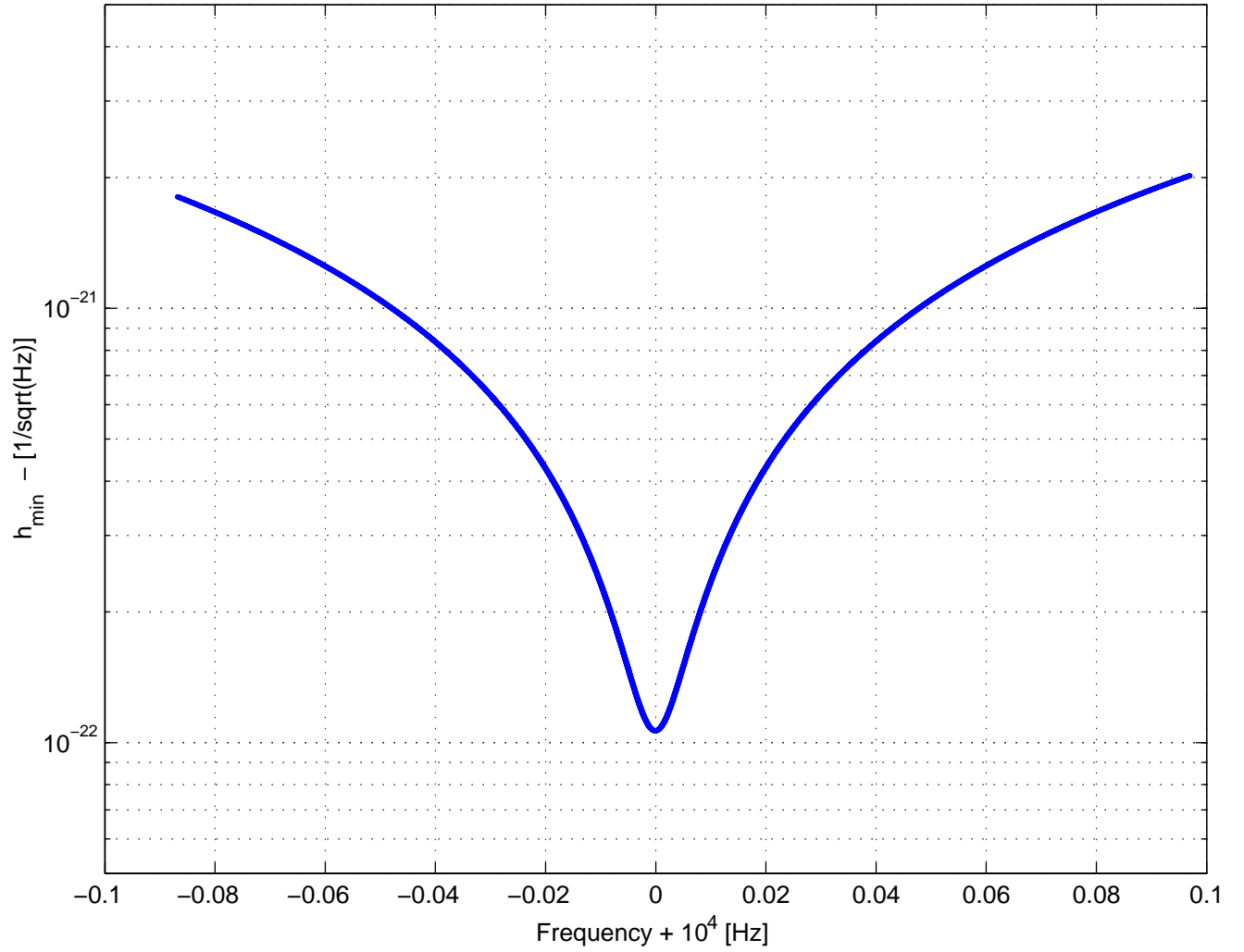


FIG. 12: Calculated large-scale system sensitivity for a periodic source ($\omega_m \approx 1$ kHz, $\omega_2 - \omega_1 = 10$ kHz, $Q = 10^{10}$, $Q_m = 10^6$, $T = 1.8$ K, $T_{eq} = 1$ K).